The EMBO Journal (2012) 31, 2103–2116 | © 2012 European Molecular Biology Organization | All Rights Reserved 0261-4189/12
www.embojournal.org

THE EMBO JOURNAL

HIF1α induced switch from bivalent to exclusively glycolytic metabolism during ESC-to-EpiSC/hESC transition

Wenyu Zhou[1,2], Michael Choi[2,3], Daciana Margineantu[4], Lilyana Margaretha[2,5], Jennifer Hesson[2,6], Christopher Cavanaugh[2,6], C Anthony Blau[2,7], Marshall S Horwitz[2,8], David Hockenbery[4,*], Carol Ware[2,6,*] and Hannele Ruohola-Baker[1,2,3,*]

[1]H Ruohola-Baker Department of Biology, University of Washington, Seattle, WA, USA, [2]Institute for Stem Cell and Regenerative Medicine (ISCRM), Seattle, WA, USA, [3]Department of Biochemistry, University of Washington, Seattle, WA, USA, [4]Fred Hutchinson Cancer Research Center, Seattle, WA, USA, [5]Molecular and Cellular Biology Program, University of Washington, Seattle, WA, USA, [6]Department of Comparative Medicine, University of Washington, Seattle, WA, USA, [7]Division of Hematology, University of Washington, Seattle, WA, USA and [8]Department of Pathology, University of Washington, Seattle, WA, USA

The function of metabolic state in stemness is poorly understood. Mouse embryonic stem cells (ESC) and epiblast stem cells (EpiSC) are at distinct pluripotent states representing the inner cell mass (ICM) and epiblast embryos. Human embryonic stem cells (hESC) are similar to EpiSC stage. We now show a dramatic metabolic difference between these two stages. EpiSC/hESC are highly glycolytic, while ESC are bivalent in their energy production, dynamically switching from glycolysis to mitochondrial respiration on demand. Despite having a more developed and expanding mitochondrial content, EpiSC/hESC have low mitochondrial respiratory capacity due to low cytochrome *c* oxidase (COX) expression. Similarly, *in vivo* epiblasts suppress COX levels. These data reveal EpiSC/hESC functional similarity to the glycolytic phenotype in cancer (Warburg effect). We further show that hypoxia-inducible factor 1α (HIF1α) is sufficient to drive ESC to a glycolytic Activin/Nodal-dependent EpiSC-like stage. This metabolic switch during early stem-cell development may be deterministic.

The EMBO Journal (2012) **31,** 2103–2116. doi:10.1038/emboj.2012.71; Published online 23 March 2012
Subject Categories: development; cellular metabolism
Keywords: human embryonic stem cell; hypoxia-inducible factor 1 alpha; metabolism; mouse embryonic stem cell; mouse epiblast stem cell

*Corresponding author. H Ruohola-Baker, Department of Biochemistry, University of Washington, 815 Mercer Street, Seattle, WA 98195, USA. Tel.: +1 206 543 8468; Fax: +1 206 685 1357;
E-mail: hannele@u.washington.edu or D Hockenbery, dhockenb@fhcrc.org or C Ware, cware@u.washington.edu

Received: 2 November 2011; accepted: 28 February 2012; published online: 23 March 2012

Introduction

Pluripotent embryonic stem cells (ESC) are able to self-renew and differentiate into the three germ lineages. Unravelling the developmental mechanisms through which pluripotency is maintained holds tremendous promise for understanding early animal development as well as developing regenerative medicine and cell therapies. Mouse and human ES cells are isolated from the inner cell mass (ICM) of pre-implantation embryos (Evans and Kaufman, 1981; Brook and Gardner, 1997; Thomson *et al*, 1998), while epiblast stem cells (EpiSC) represent cells from the post-implantation epiblast, a later stage in development (Tesar *et al*, 2007). ESC and EpiSC are pluripotent, yet display distinct features in terms of gene expression, epigenetic modifications and developmental capacity following blastocyst injection. Though isolated from the ICM, human embryonic stem cells (hESC) are similar to EpiSC based on transcriptional and protein expression profiles and their epigenetic state. Thus, pluripotency does not represent a single defined state; subtle stages of pluripotency, with similarities and differences in measurable characteristics relating to gene expression and cellular phenotype, provide an experimental system for studying potential key regulators that constrain or expand the developmental capacity of ESC.

ESC, often termed naive pluripotent cells (Nichols and Smith, 2009), efficiently contribute to chimeric embryos, maintain both X chromosomes in an active state (XaXa) in female cells, and are relatively refractory in their potential to differentiate into primordial germ cells (PGCs) *in vitro*. EpiSC and hESC, primed pluripotent cells, can give rise to differentiated teratomas, but EpiSC are highly inefficient in repopulating the ICM upon aggregation or injection into host blastocysts. These cells have variable and at times abnormal X-chromosome inactivation status (XiXa), and are poised for differentiation into PGC precursors *in vitro* (Brons *et al*, 2007; Tesar *et al*, 2007; Hayashi and Surani, 2009). Naive ESC can be cloned with high efficiency as packed domed colonies, and are stabilized by LIF/Stat3 (Smith *et al*, 1988). In contrast, EpiSC and hESC are characterized by flat colony morphology, relative intolerance to passaging as single cells, and a dependence on bFGF and TGFβ/Activin signalling rather than LIF/Stat3 (James *et al*, 2005; Bendall *et al*, 2007; Greber *et al*, 2010).

In order to understand how these pluripotent cells maintain their distinct abilities to self-renew and differentiate, global gene expression, epigenetic modification and protein expression profiling have been employed to identify key regulators. Despite significant advances using these approaches, the framework defining pluripotency in stem cells remains incompletely understood. This is in part due to the difficulty of correlating expression data with functional activity. Given that the function and integrity of a cell are affected by primary metabolism, a promising complementary

approach is to directly explore the metabolic signatures that reflect the integrated function of multiple pathways operating within cells.

In the current study, we evaluated the bioenergetic profiles of ESC, hESC and EpiSC with respect to mitochondrial DNA (mtDNA) copy number, cellular ATP levels, oxygen consumption rate (OCR) and extracellular acidification rate (ECAR). We show that while ESC are metabolically bivalent, EpiSC and hESC are almost exclusively glycolytic. We further show that hypoxia-inducible factor 1α (HIF1α) is an important regulator in the metabolic and functional transition from ESC to EpiSC. These results demonstrate a significant relationship between metabolic phenotype and pluripotent developmental stage that correlates with the underlying stem-cell functional biology.

Results

EpiSC and hESC are metabolically distinct from ESC

To characterize the metabolic profiles of ESC, EpiSC and hESC, we initially measured two metabolic parameters: OCR and ECAR under various conditions and treatments using three different experimental systems (SeaHorse Extracellular Flux analyzer, Figure 1; Perifusion Flow System and Perifusion Microscopic System, Supplementary Figure 1). OCR mainly measures the level of mitochondrial respiration. ECAR correlates with glycolytic activity, since the major exported acid, lactic acid, is derived from pyruvate generated through glycolysis, recycling NADH to NAD^+ for utilization in glycolysis. We used two representative cell lines for each pluripotency stage (ESC: R1 and G4; EpiSC: EpiSC#5 and EpiSC#7; and hESC: H1 and H7), and measured the baseline OCR of these cells in minimal medium. Interestingly, we found that both EpiSC and hESC have low basal OCRs (normalized to cell number or protein level; Supplementary Table 4) compared with ESC (Figure 1A and C). In the presence of glucose, the ECARs for EpiSC and hESC are substantially higher than for ESC (Figure 1B, E and F). This observation indicates a strong preference of EpiSC and hESC for glycolytic metabolism. The ECAR difference in ESC and EpiSC was confirmed by direct measurement of lactate levels in conditioned media (Figure 2A). The ECAR difference could also partially result from other possible acid generation, including monocarboxylates and CO_2 produced from respiration. Furthermore, carbonyl cyanide 3-chlorophenylhydrazone (CCCP) was added in order to discharge the proton gradient thereby allowing maximal turnover of the electron transport chain (ETC) uncoupled from ATP synthesis. This analysis allows estimation of the maximal mitochondria reserve in the presence of glucose (Goldsby and Heytler, 1963; Heytler, 1963). A robust increase in OCR was detected in ESC in the presence of CCCP (Figure 1A and D; Supplementary Figure 1A and B). However, very little or no increase in OCR was observed with EpiSC or hESC (Figure 1A and D; Supplementary Figure 1A and B), indicating that these cell types have diminished mitochondrial functional reserves. The observed change in ECAR due to CCCP administration could be due to increased glycolysis, or increased CO_2 production from the TCA cycle. From calculations based on OCR and ECAR changes upon glucose addition, we further show that ATP production upon glucose addition is higher in EpiSC and hESC than in ESC (Figure 1G), probably reflecting a higher glycolytic capacity in these cells. In contrast, cellular ATP content is lower in EpiSC than in ESC (Figure 1H), suggesting a high ATP consumption rate in EpiSC. To compare different stages of ES cells in human, we used hESC H1 cells treated with sodium butyrate as a developmentally earlier stage (Ware *et al*, 2009). We observed that, similar to EpiSC, hESC H1 cells contain a lower steady-state level of ATP compared with an earlier pluripotent stage (Supplementary Figure 2A). Taken together, these results demonstrate a clear metabolic difference between ESC as compared with EpiSC and hESC: the latter two cells are alike in terms of having lower mitochondrial respiration and higher glycolytic rate. These differences raise interesting questions as to how these metabolic changes occur and the impact of these differences on cellular pluripotency.

EpiSC and hESC are highly glycolytic

To further test the requirement for glycolysis in the two pluripotent stages, we cultured ESC, EpiSC and hESC with 2-deoxyglucose (2-DG), a glucose analogue that competes with glucose as a substrate for glycolytic enzymes and therefore acts as an inhibitor of glycolysis. In the presence of 2-DG, we observed that ESC grow more slowly, but maintain an ESC phenotype, forming domed cell colonies that stain with alkaline phosphatase (Figure 2B). However, EpiSC and hESC cannot survive in the presence of 2-DG (Figure 2B). In EpiSC and hESC, ECAR decreases to a greater extent than in ESC with addition of 2-DG (Figure 2C), however, unlike ESC, the ability to increase respiration to compensate for decreased glycolysis is greatly diminished at the EpiSC stage (in both EpiSC and hESC). A similar effect was observed using a lactate dehydrogenase inhibitor, oxamate (Figure 2D). In the presence of oxamate, pyruvate generated by glycolysis cannot be converted to lactate, but may be available for mitochondrial oxidation in the citric acid cycle, leading to an increase in mitochondrial respiration as observed in ESC. Our results showed that no increase in OCR was observed for EpiSC and hESC (Figure 2D). Taken together, these results indicate that glycolysis is essential for EpiSC and hESC bioenergetics due to their low mitochondrial respiratory capacity.

EpiSC and hESC have more mature mitochondria but lower mitochondrial respiration than ESC

Several additional lines of evidence further confirm that EpiSC and hESC have reduced mitochondrial respiration as compared with ESC. Treatment of these cells with oligomycin, an ATP synthase inhibitor (Chappell and Greville, 1961), resulted in similar residual OCR for ESC, EpiSC and hESC (Figure 3A). Since inhibition of mitochondrial ATP synthesis results in similar residual OCR, the higher OCR in ESC can be attributed to a higher level of coupled mitochondrial respiration. FCCP treatment following oligomycin resulted in higher OCR increase in ESC than in EpiSC and hESC (Figure 3A), confirming a higher level of maximal mitochondrial activity in ESC. Another mitochondrial uncoupler, 2,4-dinitrophenol (DNP) (Krahl and Clowes, 1936) also gave similar results to CCCP (Figure 3B).

Lower mitochondrial respiration in EpiSC and hESC could be due to reduced numbers of mitochondria or reflect the developmental immaturity of mitochondria in these cells compared with ESC. To test this, we first examined

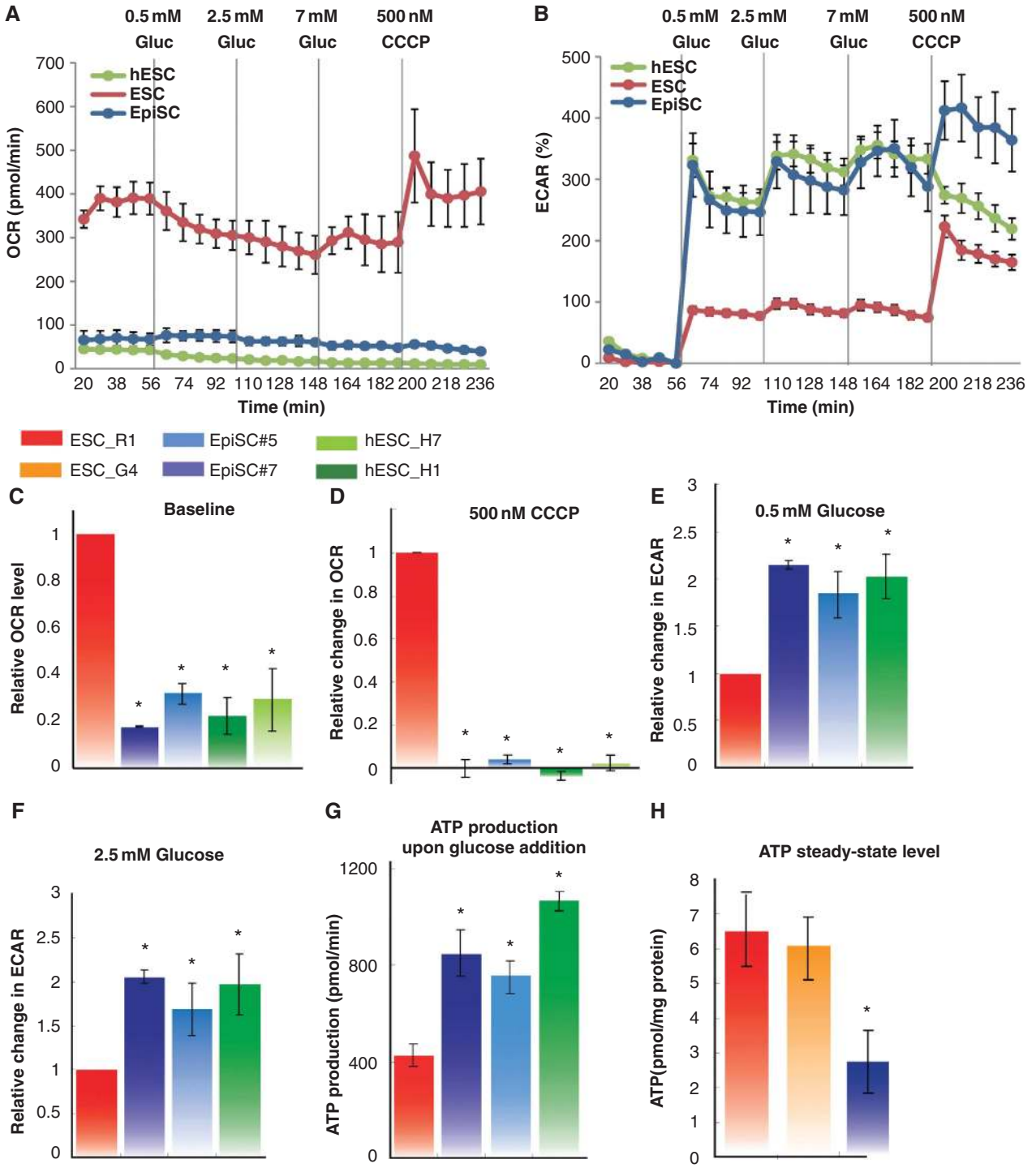

Figure 1 EpiSC and hESC show similar metabolic profiles. EpiSC and hESC have lower mitochondrial respiration activity and higher glycolytic rate than ESC. Oxygen consumption rate (OCR) (**A**, **C**, **D**) and extracellular acidification rate (ECAR) (**B**, **E**, **F**) measured in SeaHorse Extracellular Flux assay are shown. To test energetic preference when glucose is present, 0.5 mM glucose, 2.5, 7 mM glucose and 500 nM CCCP, a mitochondria uncoupler, were injected during the experiment with the same time intervals; (**A**) and (**B**) are traces from a representative SeaHorse run. (**G**) ATP production was calculated directly from OCR and ECAR measured in SeaHorse assay following ATP produced = OCR × time course × 5 + ECAR × time course. (**H**) ESC have higher ATP content as the steady-state level than EpiSC. Results were summarized from at least three independent biological experiments, each consisting of independent cell plating on five SeaHorse microplate wells. The error bars represented the standard error of the mean, as calculated by sample standard deviation divided by the square root of the sample size. *Indicates $P<0.05$.

morphology of mitochondria in EpiSC and hESC compared with ESC by electron microscopy. We observed that the majority of mitochondria in ESC are rounded to oval, displaying sparse and irregular cristae and an electron-lucent matrix, in contrast to the mitochondria of EpiSC and hESC, which are more elongated, and contain well-defined transverse cristae and a dense matrix (Figure 3C–E). Elongated mitochondria were observed about three and five times as

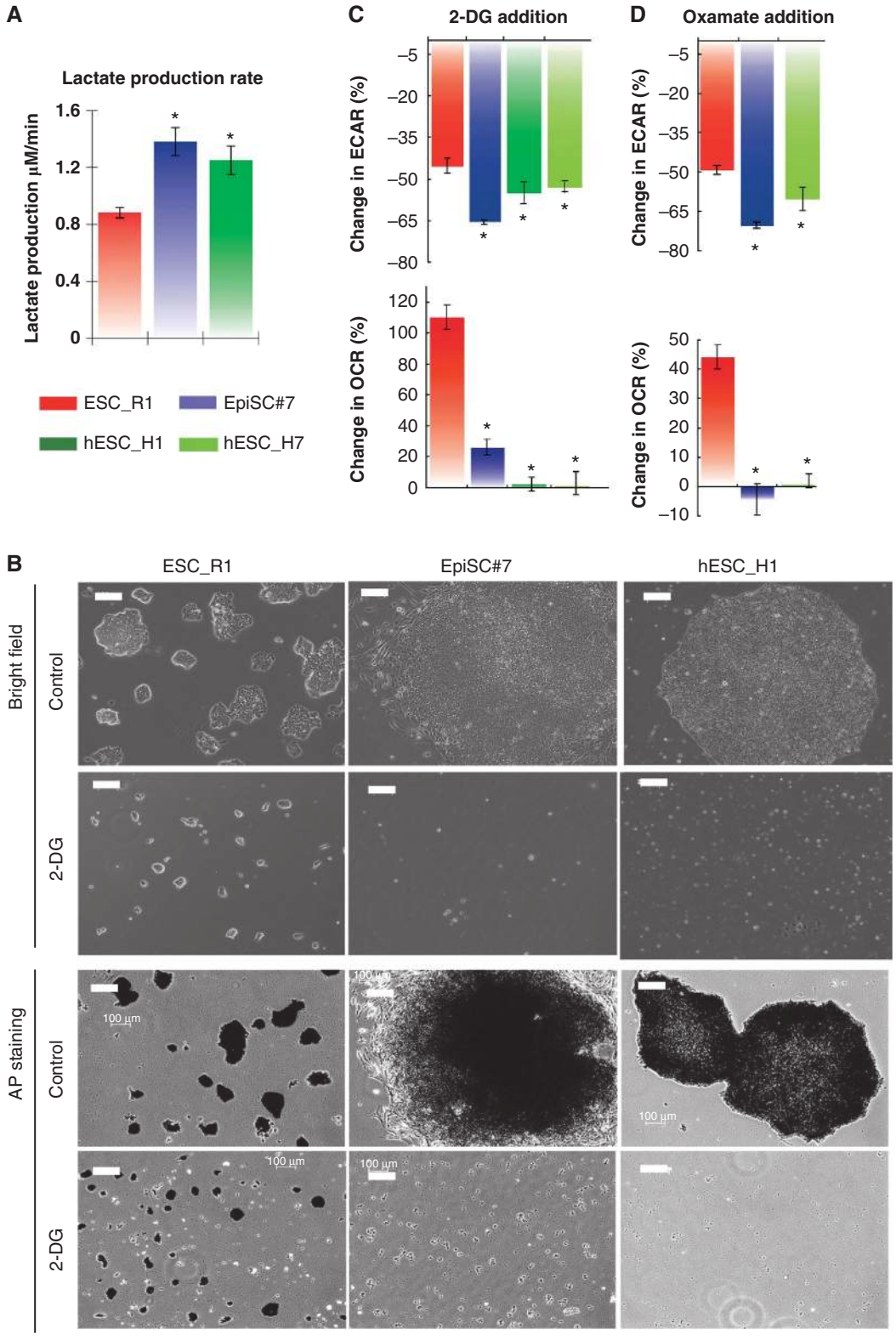

Figure 2 EpiSC are highly glycolytic compared with ESC. (**A**) EpiSC produce higher level of lactate, indicative of higher pyruvate generated through glycolysis. (**B**) ESC retain pluripotency in the presence of 2-deoxyglucose (2-DG), while EpiSC and hESC die upon 2-DG addition; Images for both bright fields and alkaline phosphatase (AP) staining are shown. (**C**) 2-DG results in higher ECAR reduction but lower OCR increase in EpiSC and hESC than in ESC, confirming the high glycolysis and low mitochondria reserve present in EpiSC. (**D**) The addition of Oxamate, an inhibitor of lactate dehydrogenase, results in higher ECAR reduction but lower OCR increase in EpiSC and hESC than in ESC, confirming the high glycolysis and low mitochondria reserve present in EpiSC. We did not observe differential expression of glucose transporters with significant trend in EpiSC compared with ESC (Supplementary Table 5), suggesting that the difference in glycolytic activity between EpiSC and ESC is not caused by glucose transporters levels. Results were summarized from two independent experiments, each consisting of independent cell plating on five SeaHorse microplate wells. The error bars represented the standard error of the mean. *Indicates $P<0.05$.

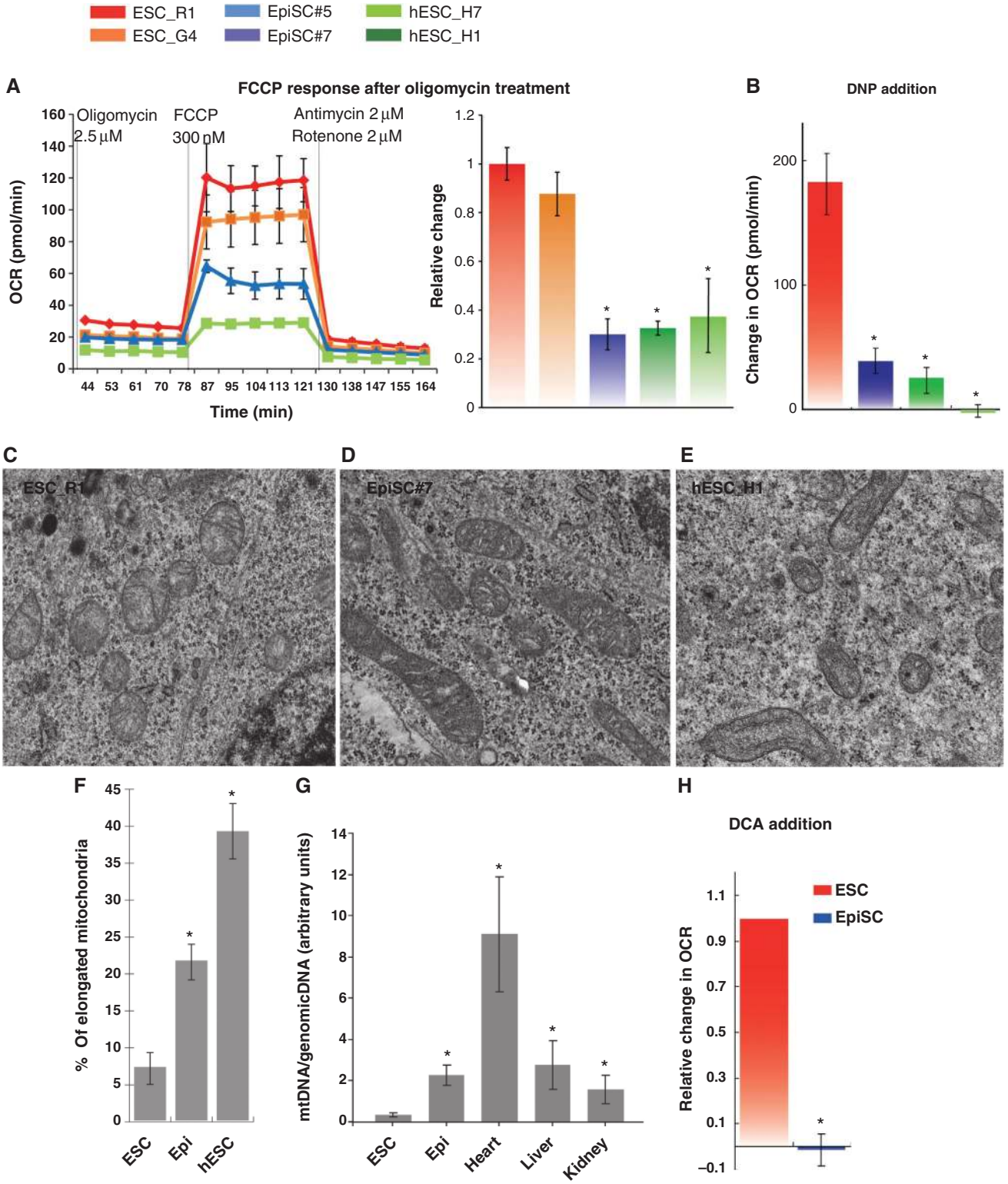

Figure 3 Lower mitochondrial respiration in EpiSC, compared with ESC, is not due to mitochondrial immaturity, low mitochondria number or lack of pyruvate accessibility to mitochondria. (**A**) The differences in OCR between ESC, EpiSC and hESC were abolished when oligomycin was present, confirming that the difference in the aerobic respiration was caused by difference in the oxidative phosphorylation. FCCP treatment following oligomycin resulted in higher OCR increase in ESC than in EpiSC and hESC, confirming the higher level of mitochondrial electron transport chain (ETC) activity in ESC. (**B**) Another mitochondrial uncoupler 2,4-DNP confirms that EpiSC and hESC have lower mitochondrial activity. Results were summarized from two independent experiments, and the error bars represented the standard error of the mean. (**C**–**F**) Electron microscopy shows that EpiSC and hESC contain more elongated mitochondria than ESC; 20 EM images containing 194 and 296 mitochondria were used, respectively, for ESC and EpiSC mitochondrial quantification, and 30 images containing 212 mitochondria were used for hESC mitochondrial quantification. (**G**) EpiSC and hESC have higher mitochondrial DNA copy number than ESC. (**H**) ESC but not EpiSC increase OCR in response to DCA. SeaHorse results were summarized from two independent experiments, each consisting of independent cell plating on five SeaHorse microplate wells. The error bars represented the standard error of the mean. *Indicates $P<0.05$.

frequently in EpiSC and hESC, respectively, as compared with ESC (Figure 3F). This morphological assessment suggests that the mitochondria of EpiSC and hESC are more mature in appearance than ESC, consistent with their relatively later developmental stage. Similarly, significantly higher mtDNA copy numbers were detected in EpiSC compared with ESC (Figure 3G), mtDNA copy number was also lower in hESC H1 cultured with sodium butyrate compared with H1 (Supplementary Figure 2B). These results stand in stark contrast to the lower respiratory activity of EpiSC and hESC relative to ESC. We also tested the possibility that diminished pyruvate oxidation by mitochondrial pyruvate dehydrogenase in EpiSC may cause the differences in mitochondrial respiration compared with ESC. Treatment with dichloroacetate, an inhibitor of pyruvate dehydrogenase kinases (Whitehouse *et al*, 1974), increased respiration in ESC, but not in EpiSC (Figure 3H).

Reduced mitochondrial respiration in EpiSC and hESC is attributable to a deficiency in ETC complex IV cytochrome c oxidase

In a search for other possible mechanisms accounting for the low mitochondrial respiration activity in EpiSC/hESC, we observed that EpiSC have lower mitochondrial membrane potential than ESC as measured by staining with tetramethylrhodamine methyl ester (TMRM) (Figure 4A), a dye that rapidly and reversibly equilibrates across membranes in a voltage-dependent manner (Ehrenberg *et al*, 1988). In agreement with a recent study (Folmes *et al*, 2011), we also observed that mouse embryonic fibroblasts (MEFs) have less TMRM staining than ESC. Lower mitochondrial membrane potential seen in EpiSC suggests that the mitochondrial ETC may not operate sufficiently to generate an effective proton gradient. In order to identify mechanisms in mitochondrial ETC that could account for the lower membrane potential of EpiSC compared with ESC, we examined gene expression microarray data from these two types of cells (Tesar *et al*, 2007), and surprisingly, found that a majority of genes in mitochondrial complex I and IV are expressed at a lower level in EpiSC compared with ESC (Figure 4B; Supplementary Figure 3A and C). Notably, in the complex IV cytochrome *c* oxidase (COX) family, 20 out of a total of 22 nuclear-encoded genes are downregulated in EpiSC ($P<0.005$; Figure 4B). We further validated the significant reduction of key genes in these ETC components in EpiSC compared with ESC by quantitative PCR assay (Figure 4C), and compared the expression abundance of these key genes as compared with β-actin in mouse and human (Supplementary Table 1). Given the uniformly reduced expression of COX mRNAs in EpiSC, it is possible that translation and assembly of COX proteins are largely defective. To test whether COX activity is deficient in EpiSC and hESC, we prepared mitochondrial extracts from ESC and EpiSC, as well as two hESC lines, H1 and H7, to measure the COX activity *in vitro*. Indeed, there is about 40% reduction in COX activity per microgram of mitochondrial protein in EpiSC as compared with ESC (Figure 4D). We also observed that hESC resemble EpiSC in having a low level of COX activity (Figure 4D). Since complex IV levels are limiting and have previously been shown to tightly regulate mitochondrial respiratory capacity (Villani *et al*, 1998), low complex IV activity in EpiSC and hESC could explain their low mitochondrial respiration activity relative to ESC.

We further found that expression of synthesis of cytochrome *c* oxidase 2 (SCO2), peroxisome proliferator-activated receptor γ coactivator-1β (PGC-1β) and oestrogen receptor-related receptor β (Esrrb, or ERR-β) is significantly lower in EpiSC as compared with ESC (Figure 4E). SCO2 is required for the assembly of the COX complex IV and mutation of this gene in humans results in fatal cardioencephalomyopathy due to mitochondrial respiratory failure (Papadopoulou *et al*, 1999) (other mitochondrial assembly factors were also examined in Supplementary Table 2). Similarly, PGC-1β controls mitochondrial oxidative metabolism by activating specific target genes that are key components of mitochondria, including those in the mitochondrial membrane and ETC (Lelliott *et al*, 2006; Sonoda *et al*, 2007). More specifically, PGC-1β could act as a ligand for Esrrb to control metabolism and energy balance (Kamei *et al*, 2003). Lower expression of SCO2, PGC-1β and *Esrrb* in EpiSC could contribute to the reduced mitochondrial respiration activity in these cells compared with ESC.

Lower mitochondrial COX genes in post-implantation epiblast in vivo

To test whether the metabolic differences between ESC and EpiSC reflect differences that exist *in vivo*, we compared our cell culture results with results obtained from high-throughput deep sequencing of mRNA using the freshly dissected ICM of pre-implantation embryos and the epiblast of post-implantation embryos (Figure 5) (manuscript in preparation). In agreement with results of ESC and EpiSC cultured *in vitro*, our deep RNA-sequence results reveal a significantly lower level of COX mRNA in the epiblast relative to the ICM (Figure 5A and B, *in vivo*: $P<0.05$, *in vitro*: $P<0.01$ as compared with all other genes). Further, close examination reveals high correlation in the most significantly downregulated COX genes (Figure 5C) and their regulators, PGC-1β and *Esrrb in vivo* versus *in vitro* (Figure 5D). These data confirm a dramatic downregulation of mitochondrial COX genes during the transition from ICM to epiblast *in vivo*.

HIF1α is a key regulator of the pluripotent state

To understand the drivers of the acquisition of a highly glycolytic state in EpiSC, we searched gene expression signatures in *in vitro* microarray data and identified the characteristic HIF1α-driven gene expression profile in EpiSC but not in ESC (Supplementary Table 3). We validated three of the key HIF1α targets, *PDK1*, *LDHA* and *PYGL*, in EpiSC compared with ESC, and observed a 10- to 70-fold increase in expression levels of these HIF1α targets in the EpiSC stage (Figure 6A). As a control, we observed the expected increase of *Cer1* in EpiSC compared with the ESC stage. We further observed that HIF1α protein is present at a significantly higher level in EpiSC than in ESC (Figure 6B; Supplementary Figure 4). To test whether HIF1α is sufficient to induce the transition from ESC to EpiSC, we overexpressed or induced HIF1α in ESC transiently for 3 days in the presence of leukaemia inhibitory factor (LIF). Importantly, both expression of a non-degradable form of HIF1α by retroviral infection and induction of endogenous HIF1α by the chemical hypoxia inducer $CoCl_2$ render ESC not only morphologically but also metabolically similar to EpiSC. We show that HIF1α stabilization through both means (Figure 6C) significantly increase the percentage of EpiSC-like colonies in ESC culture

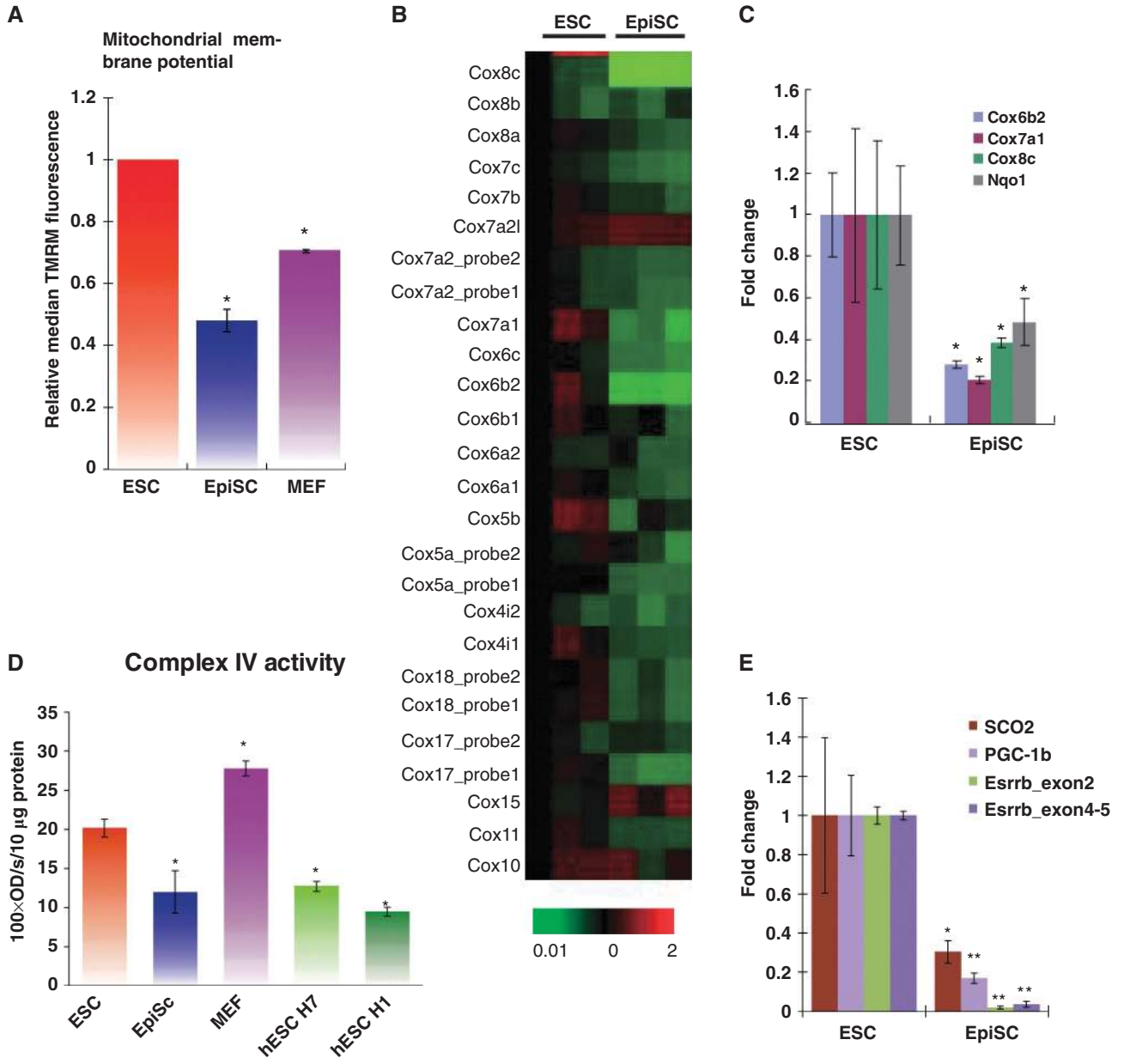

Figure 4 Expression of nuclear-encoded mitochondrial IV COX genes is lower in EpiSC compared with ESC, resulting in lower complex IV activity in EpiSC. (**A**) EpiSC have lower mitochondrial membrane potential than ESC and MEFs measured by TMRM staining. (**B**) Heatmap of microarray expression data of mitochondrial complex IV COX gene cluster is shown, where EpiSC clearly demonstrate lower expression in these genes than ESC. (**C**) Validation of *Cox8c*, *Cox6b2*, *Cox7a1* and *NqoI* by quantitative PCR assays. (**D**) Complex IV isolated from EpiSC or hESC (H1 and H7 lines) shows lower activity *in vitro* than that of ESC; the activity of Complex IV isolated from MEFs is shown as comparison. (**E**) Potential regulators involved in mitochondria respiration, SCO2, PGC-1β and *Esrrb*, express at lower levels in EpiSC. Results were summarized from three independent biological samples, and the error bars represented the standard error of the mean. *Indicates $P<0.05$, ** indicates $P<0.01$.

in the presence of LIF (Figure 6D–H). Further, HIF1α overexpressing ESC have reduced mitochondrial respiration and higher glycolytic activity compared with control ESC (Figure 6I–K). Although transient overexpression of HIF1α for 3 days did not show changes at the molecular level of key genes (data not shown), overexpression of HIF1α for a longer period (6 days) does result in significant changes in the expression level of key genes toward an EpiSC-like stage, including lineage marker *Cer1*, glycolytic gene *LDHA* and two other metabolism-related genes *Cox7a1* and *Esrrb* (Figure 6L; Supplementary Figure 5). These data suggest that HIF1α acts as a key regulator of the metabolic and phenotypic shifts from ESC to EpiSC.

Activin signalling is indispensable in the HIF-regulated transition from ESC to EpiSC

Activin is shown to be essential for maintenance of EpiSC in culture and withdrawal of Activin signalling results in EpiSC differentiation into neuroendoderm (Vallier *et al*, 2004; James *et al*, 2005; Camus *et al*, 2006). In contrast, ESC do not require Activin for pluripotency (Tesar *et al*, 2007); conversely, addition of Activin signalling results in a shift from the

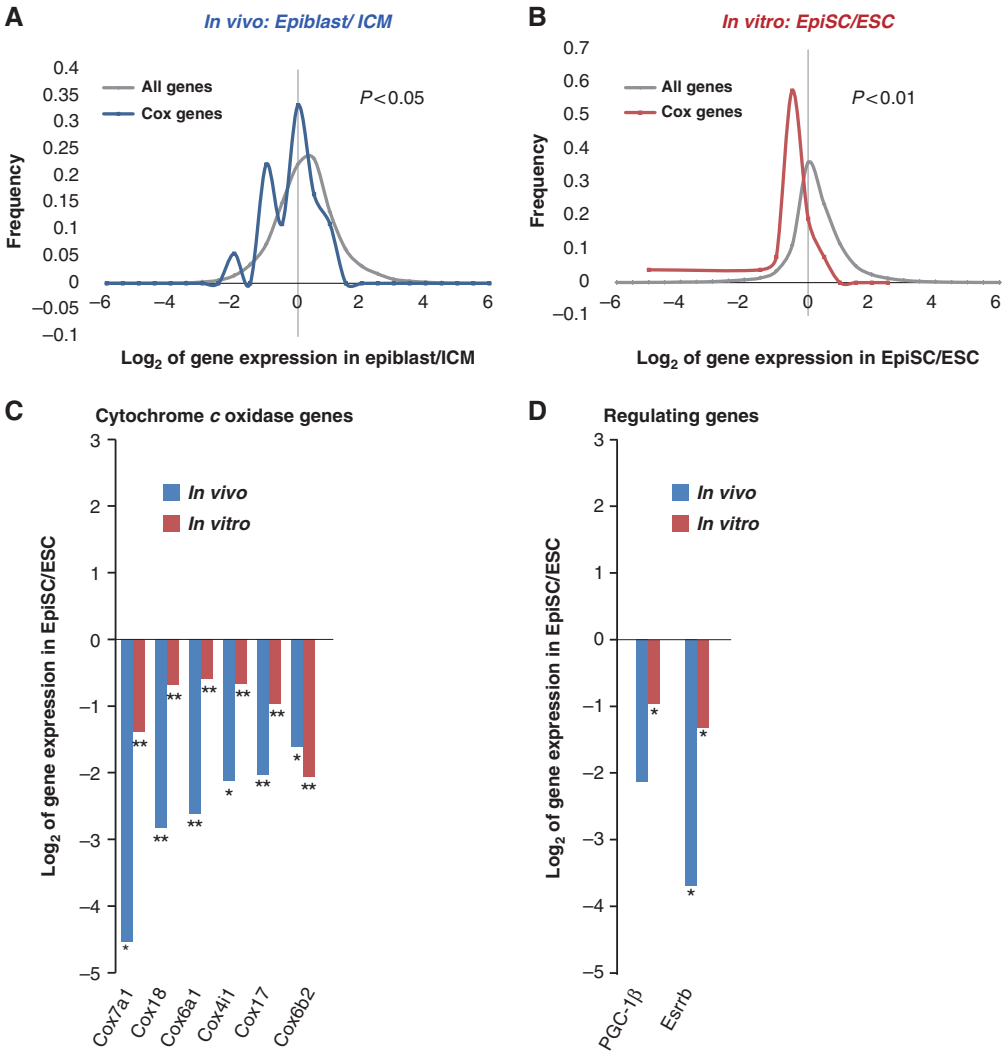

Figure 5 Deep RNA-sequence analysis of freshly dissected inner cell mass and epiblast reveals high similarity in mitochondrial COX gene expressions *in vivo* and *in vitro*. Expression levels of COX genes only are compared with that of all genes in the *in-vivo* data set (**A**) and in the *in-vitro* data set (**B**) to illustrate the downregulation of COX genes (*in vivo*: $P<0.05$; *in vitro*: $P<0.01$). (**C**) The comparison of the most significantly downregulated COX genes *in-vivo* and *in-vitro* data is shown. (**D**) High correlation of *in-vivo* and *in-vitro* data in the expression levels of PGC-1β and *Esrrb* is shown. Biological triplicates were used for each embryonic stage, the lysate comprised ~50 embryos in each experiment. *Indicates $P<0.05$, ** indicates $P<0.01$.

ESC towards EpiSC state (Guo *et al*, 2009; Hayashi *et al*, 2011; Figure 7A; Supplementary Figure 6). In this study, we show that HIF1α activation switches ESC morphologically, metabolically and based on the expression signature towards an EpiSC-like state. To test whether HIF1α regulates this state switch through Activin signalling, we cultured ESC with LIF media containing $CoCl_2$ as well as an inhibitor of Activin signalling, SB431542 (ALKi), which specifically binds with Activin receptor-like kinase (Inman *et al*, 2002). While chemical hypoxia alone induced the EpiSC-like state in 50% of the ESC colonies, no EpiSC-like induction was observed when the Activin pathway was repressed during chemical hypoxia (Figure 7A). These data show that HIF1α-dependent induction of the EpiSC state requires Activin/Nodal signalling. During Activin induced ESC-to-EpiSC transition, we observed that HIF1α protein is stabilized (Figure 7B). Furthermore, we also observed significant changes in the expression levels of key metabolic genes, including upregulation of glycolytic gene *LDHA* and downregulation of genes regulating mitochondrial activity *Cox7a1* and *Esrrb* when ESC are cultured with Activin and FGF (Figure 7C; Supplementary Figure 5). No *Cer1* upregulation was observed in ESC cultured with Activin and FGF for 3 days, even though these cells displayed an EpiSC-like metabolic signature. We therefore further analysed the kinetics of key metabolic and lineage-related genes in the course of ESC-to-EpiSC transition induced by Activin and FGF in culture (Hayashi *et al*, 2011). The analysis shows that changes in metabolic gene expression precede the changes in the expression of EpiSC lineage markers upon Activin treatment (Figure 7D). Together, these data suggest that the Activin signalling pathway is required during the ESC-to-EpiSC transition possibly by regulating key genes related to metabolism that are characteristic of the EpiSC stage.

Discussion

In the present study, we demonstrate that a dramatic switch from a bivalent metabolism to an exclusively glycolytic

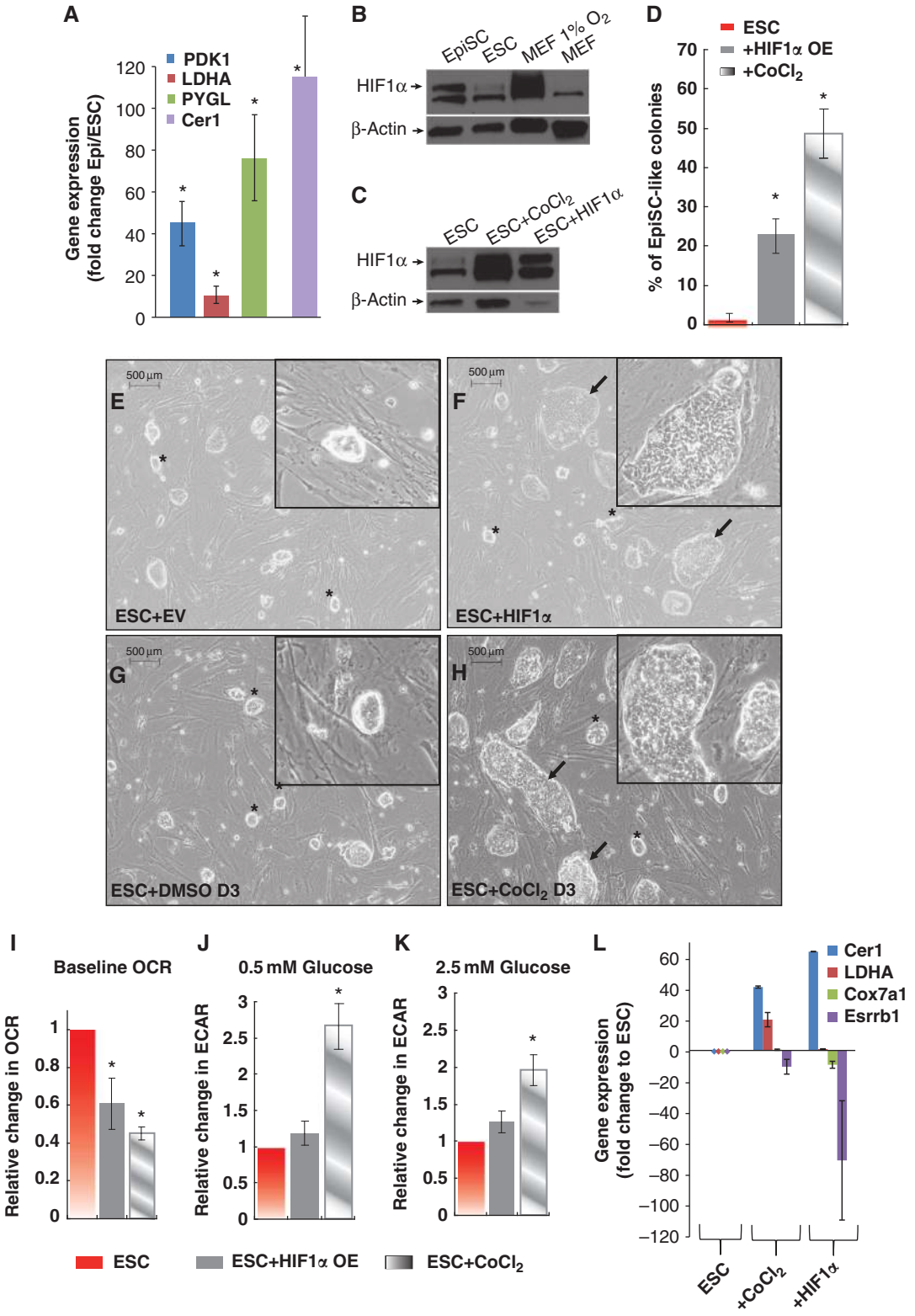

Figure 6 HIF signature is present in EpiSC as glycolysis regulator. (**A**) *PDK1*, *LDHA* and *PYGL* that are involved in glycolysis and also HIF targets are expressed at higher levels in EpiSC; *Cer1* is expected to increase in EpiSC and used in comparison. Quantitative PCR validation is shown. (**B**) EpiSC expresses HIF1α protein under 21 O_2, while little expression is shown in ESC. (**C**) HIF1α expression is confirmed in ESC treated with $CoCl_2$ and HIF1α viral expression. (**D**–**H**) HIF1α overexpressing ESC transiently for 3 days (ESC + HIF1α and ESC + $CoCl_2$D3) form flat monolayer EpiSC-like colonies (shown by arrow), which are not present in control ESC (ESC + EV empty vector and ESC + DMSO); the normal-looking ESC labelled by stars and quantification of the percentage of EpiSC-like colonies are shown; ESC + HIF1α and ESC + $CoCl_2$ are metabolically different from ESC by having (**I**) lower baseline OCR and higher ECAR increase upon both 0.5 mM glucose (**J**) and 2.5 mM glucose addition (**K**), resembling EpiSC. (**L**) Significant changes resembling EpiSC in *Cer1*, *LDHA*, *Cox7a1* and *Esrrb* expression were observed in ESC + HIF1α and ESC + $CoCl_2$. Results were summarized from two independent experiments, each consisting of independent cell plating on five SeaHorse microplate wells. The error bars represented the standard error of the mean. *Indicates $P<0.05$.

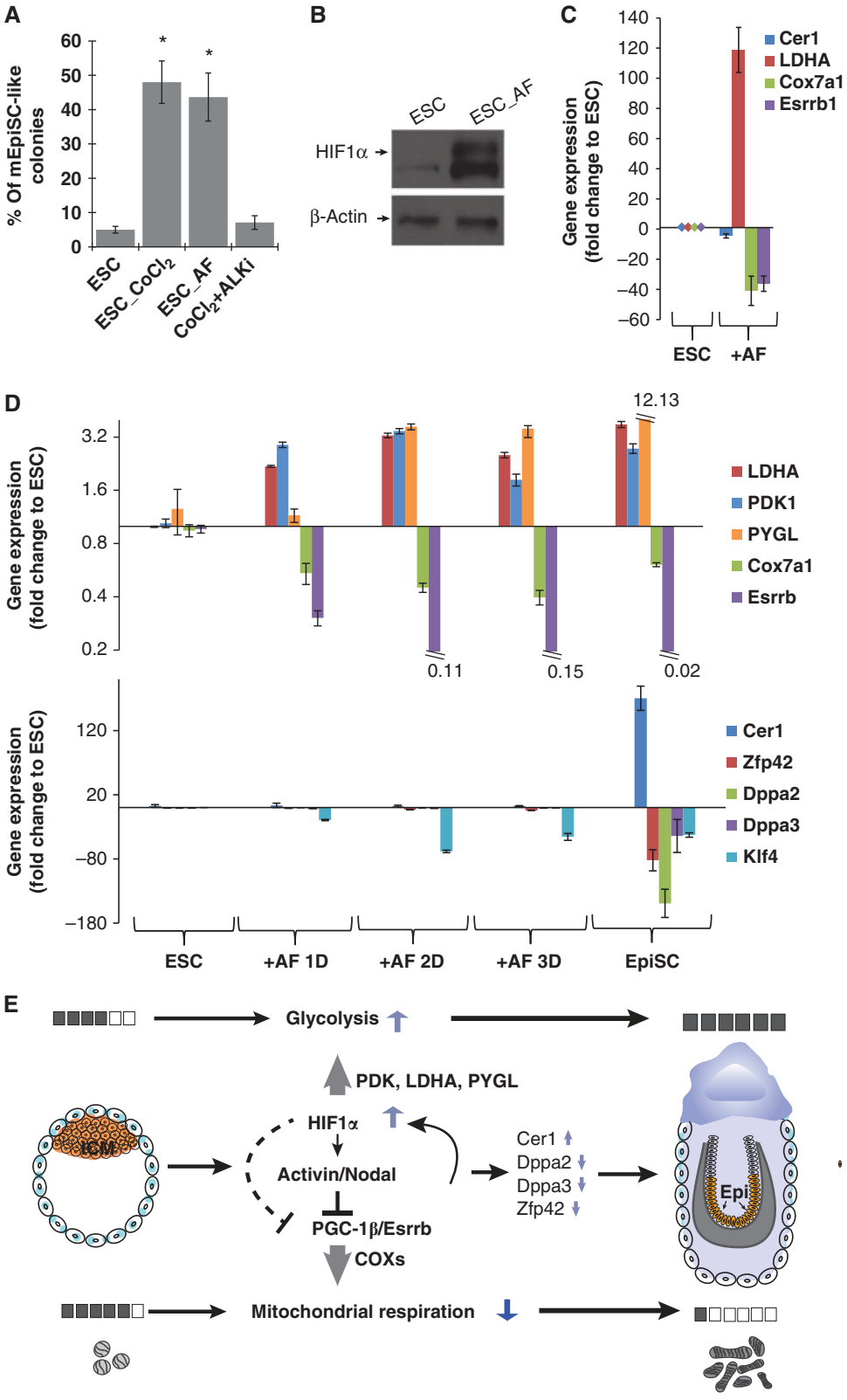

Figure 7 (**A**) Quantification of the percentage of EpiSC-like colonies in ESC, ESC + $CoCl_2$, ESC + Activin and ESC + $CoCl_2$ + ALKi shows that Activin/Nodal signalling is required for $CoCl_2$ induced ESC-to-EpiSC transition. (**B**) ESC + Activin express HIF1α as confirmed by western blot. (**C**) Significant changes resembling EpiSC in *LDHA*, *Cox7a1* and *Esrrb* expression were observed in ESC + Activin. (**D**) Expression kinetics are shown for key metabolic genes (*LDHA*, *PDK1*, *PYGL*, *Cox7a1* and *Esrrb*) and lineage-related genes (*Cer1*, *Zfp42*, *Dppa2*, *Dppa3* and *Klf4*) in ESC-to-EpiSC transition induced by Activin and FGF in culture, microarray from Hayashi *et al* was examined. (**E**) Illustration of the regulatory network in the metabolic transition from ESC to EpiSC: higher HIF activity in EpiSC increases glycolysis. HIF downregulates PGC-1β expression, reducing COX expression and ultimately resulting in a low mitochondrial respiration in EpiSC.

metabolism takes place between two pluripotent stages reflective of the pre-implantation ICM and post-implantation epiblast (Figure 7E). While ESC possess functional mitochondrial respiration in minimal media and upon extrinsic induction, EpiSC and hESC are defective in mitochondrial function, mainly relying on glycolysis for cellular ATP demand. We found that EpiSC and hESC show low mitochondrial ETC complex IV activity, compromising the overall respiratory capacity of these cells. The downregulation of complex IV in ICM to epiblast transition is also observed *in vivo*, suggesting that the ETC downregulation in the epiblast stage has a tremendous beneficial value for the pluripotent cell population. Furthermore, EpiSC and hESC upregulate key glycolytic genes, maximizing their anaerobic capacity to fulfil cellular energy demand.

Metabolic changes are associated with cellular differentiation. The choice between anaerobic metabolism and aerobic respiration may play an important role in determining specific lineage decisions (Roberts *et al*, 2009; Bracha *et al*, 2010; Yanes *et al*, 2010; Mandal *et al*, 2011). Among other changes, the number, morphology and function of mitochondria dramatically change at different developmental stages. In early embryo development, mitochondria in the 8-cell embryo reveal minimal matrix electron density. Elongating mitochondria with inner mitochondrial membranes arranged into transverse cristae appear, and the replication of mtDNA takes place in expanding blastocysts (Sathananthan and Trounson, 2000; Thundathil *et al*, 2005). It has been shown previously that undifferentiated ESC, compared with their differentiated progeny, have restricted oxidative capacity with low mtDNA copy number and low mitochondrial mass (Cho *et al*, 2006). Consistent with these previous findings, our data show that compared with ESC, the advanced pluripotency state reflected in EpiSC leads to more mature mitochondria and higher mtDNA copy numbers. However, paradoxically we found that mitochondria in EpiSC are less active, and defective in aerobic respiration due to compromised COX activity. Low COX gene expression and low mitochondrial respiration are conserved in hESC, suggesting that low mitochondrial activity is beneficial for cells at this stage. One possibility is that since the PGC precursors—which are a necessity for the continuity of the species—are formed at the epiblast stage, the developing animal will minimize the potential harm generated by reactive oxygen species by blocking mitochondrial activities to protect the germ line. Recent findings support this hypothesis. Activin treatment for a short period of time induces ESC to a stage potent for PGC differentiation (Hayashi *et al*, 2011). These cells show an EpiSC-like metabolic signature, however, they do not show yet the canonical fate marker changes observed in EpiSC (Figure 7D), suggesting that the metabolic changes may be imperative for successful PGC formation.

COX activity has been shown to be a rate limiting factor in mitochondrial respiration (Villani *et al*, 1998). The degradation of mitochondrial function through loss of COX activity is also evident in several pathological cases. COX is a specific intra-mitochondrial site of age-related deterioration (Dillin *et al*, 2002; Ren *et al*, 2010), and is currently considered as an endogenous marker of neuronal oxidative metabolism (Bertoni-Freddari *et al*, 2004), which when defective may be causal for Alzheimer's disease (Ojaimi *et al*, 1999). In the present study, we demonstrate that while EpiSC/hESC have a robust number of maturing mitochondria, the expression of COX genes is downregulated, reducing the mitochondrial function in EpiSC/hESC. This work through defining the metabolic differences between two pluripotent stages has revealed that the developing animal can modulate mitochondrial activity by regulating COX levels. While reduction of COX activity is previously shown to associate with pathological cases, the developing pluripotent stem cell can harness this reduction to its benefit, possibly to protect its pluripotent stage against oxidative stress. It will be important to reveal whether this same strategy is used in other developmental stages.

The PGC-1 family is involved in regulating mitochondrial activity. Compared with ESC, we found that EpiSC show lower expression of PGC-1β, as well as ERR-β, the nuclear receptor it coactivates. Reduced expression of PGC-1β combined with ERR-β has been shown to result in reduced ERR-mediated transcription of nuclear-encoded mitochondrial genes, which would ultimately attenuate mitochondrial function (Shao *et al*, 2010). Direct comparison using microarray analysis reveals increased expression of PGC-1α in EpiSC (Supplementary Table 1), which is in accordance with its known role regulating mitochondrial biogenesis and replication (Wu *et al*, 1999) and could explain the increased mitochondria content observed in EpiSC. A critical aspect of PGC-1 co-activators is that they are highly versatile; PGC-1α and β are shown to interact with members of the nuclear receptor superfamily, as well as distinct transcription factors outside of the super family (Lin *et al*, 2005). We speculate that in early embryonic development, PGC-1 members play different and crucial roles in mitochondrial biology: PGC-1α may regulate mitochondrial replication and biogenesis by activating mitochondrial and nuclear transcription, and the lack of PGC-1β may play a role in repressing the function of these newly generated mitochondria. Overall, the coordinated regulation by PGC-1 enables early embryonic cells to develop a sufficient number of mitochondria as a reservoir for the increased energy demands for future differentiation, while maintaining an anaerobic metabolism important for self-renewal and pluripotency (Varum *et al*, 2009; Gan *et al*, 2010).

Embryonic development takes place in a hypoxic environment (Fischer and Bavister, 1993; Lee *et al*, 2001), and HIF1α signalling has been shown to play an indispensable role in directing morphogenesis in the embryo and placenta (Dunwoodie, 2009). We have shown that HIF1α can play a role in pluripotency by regulating metabolic transition of the pluripotent cells before and after implantation. We demonstrate that HIF1α overexpression not only induces morphological change reflective of the transition from ESC to EpiSC, but is also sufficient to enhance glycolysis at the expense of oxidative phosphorylation. These observations are consistent with the known function of HIF1α in glycolysis (Seagroves *et al*, 2001). Moreover, HIF1α can induce active suppression of mitochondrial oxidative respiration. We observe lower mitochondrial respiratory activity in EpiSC, and HIF1α overexpression in ESC phenocopies this metabolic shift.

We further reveal that metabolic changes during the ESC-to-EpiSC transition induced by HIF1α act through Activin/Nodal signalling. HIF1α has been shown to bind to HIF responsive element (HRE) on the Activin B promoter to directly regulate its expression (Wacker *et al*, 2009). HIF1α

induces Activin receptor-like kinase (Garrido-Martin *et al*, 2010), which further mediates some hypoxia-induced processes, such as angiogenesis (Lux *et al*, 2006). Moreover, activation of Activin/Nodal signalling is required to maintain pluripotent cells in culture as EpiSC, preventing the spontaneous differentiation process (Vallier *et al*, 2004; James *et al*, 2005; Camus *et al*, 2006), and recombinant Activin is sufficient to transit ESC towards EpiSC (Hayashi *et al*, 2011; Figure 7A; Supplementary Figure 6). It has also been shown that Activin/Nodal stabilizes HIF1α by decreasing prolyl hydroxylase 2 (Wiley *et al*, 2010). Accordingly, we observed HIF1α stabilization due to Activin induction in ESC. Given these observations, it is possible that a feedback loop exists between HIF1α and Activin/Nodal signalling during early embryonic development (Figure 7E).

We identify three transcriptional signalling pathways (PGC-1β, HIF1α and Activin/Nodal) that are involved in the dramatic metabolic change between pluripotency stages (Figure 7E). HIF1α is shown to negatively regulate PGC-1β by inhibiting c-Myc transcriptional activity (Zhang *et al*, 2007). Further, Activin/Nodal signalling is reported to affect metabolism and is suggested to directly downregulate PGC-1, downregulating mitochondrial metabolism (Li *et al*, 2009). Interestingly, the changes in metabolic gene expression precede the changes in the expression of EpiSC lineage markers upon Activin treatment, suggesting that metabolic changes may be leading the process. We propose a regulatory network that controls the proper metabolic switch in early embryo development (Figure 7E). In this network, we envision HIF1α as a master regulator: it not only plays an important role in anaerobic metabolism by activating key glycolytic enzymes, but also actively represses mitochondrial activity through inhibition of PGC-1β. Moreover, HIF1α acts through Activin/Nodal signalling, to broaden its effect by inhibiting the differentiation process and to strengthen its suppressive role in PGC-1. It remains to be answered whether such a regulatory network is conserved in human embryo development, and what other intermediate regulators are involved in this network.

Cancer cells are frequently characterized by a glycolytic shift, known as the Warburg effect. HIF-1 and Myc, transcription factors linked to the Warburg effect, are integral to ESC programs. The outcome of the Warburg effect is to increase metabolic flux of glucose carbons into biosynthetic precursors, fuelling anabolic processes, and control of redox potential and ROS that are required for rapid tumour cell growth and division. The developmental suppression of oxidative phosphorylation in EpiSC/hESC may serve a similar function in preparation for embryonic growth and formation of germ cell layers.

Materials and methods

Cell culture

Early passage (passage <40) ESC and EpiSC were cultured on irradiated MEF feeder at 37°C, as described previously (Tesar *et al*, 2007; Ying *et al*, 2008). Specifically, medium for ESC contained DMEM (Invitrogen), 15% ES cell-qualified fetal bovine serum (Atlas Biologicals), 1 mM 2-mercaptoethanol (Sigma-Aldrich), 2 mM pyruvate (Invitrogen), non-essential amino acids (Invitrogen) and 10^3 units/ml LIF (Millipore) with addition of GSK and MEK inhibitors (2i: GSKi: CHIR99021; MEKi: PD0325901, Stemgent). ESC were passaged every 2–3 days as a single-cell suspension using 0.25% trypsin/EDTA. Medium for EpiSC culture consisted of DMEM-F12 (Invitrogen), 20% knockout serum replacement (Invitrogen), 5 ng/ml FGF2 (R&D Systems), 0.1 mM 2-mercaptoethanol (Sigma-Aldrich), 2 mM pyruvate (Invitrogen), non-essential amino acids (Invitrogen) and recombinant Activin A (Humanzyme). EpiSC were passaged every 2–3 days with Dispase (Invitrogen) and triturated into small clumps. hESC were cultured as EpiSC, but without addition of Activin A.

OCR and ECAR measurements using SeaHorse Cellular Flux assays. SeaHorse plates were pre-treated by coating with 0.1% Gelatin and irradiated MEFs were seeded thereafter. About 24 h before measurement, MEFs were lysed using a detergent solution 0.5% Triton and 0.034% (v/v) NH_4OH (Sigma-Aldrich) to retain their extracellular matrix and eliminate background OCR and ECAR. Cell density titrations were performed to define the optimal seeding density for ESC (Supplementary Figure 7A) and EpiSC (Supplementary Figure 7B), and in following experiments, ESC and EpiSC were passaged and seeded in growth media described above onto pre-treated SeaHorse plates with $2–2.5 \times 10^5$ ESC or $0.8–1 \times 10^5$ EpiSC per XF24 well to ensure about 90% surface coverage at the time of the experiment. Culture media were exchanged for base media (unbuffered DMEM (Sigma D5030) supplemented with 2 mM Glutamine) 1 h before the assay and for the duration of the measurement. Substrates and selective inhibitors were injected during the measurements to achieve final concentrations of glucose (0.5, 2.5 and 7 mM), CCCP (500 nM), oligomycin (2.5 μM), 2,4-DNP (100 μM), DCA (20 mM), 2-DG (50 mM) and Oxamate (50 mM) (all from Sigma-Aldrich); and CCCP, 2,4-DNP, 2-DG and Oxamate titrations were performed (CCCP, Supplementary Figure 8A; 2-DG, Supplementary Figure 8B; Oxamate, Supplementary Figure 8C and 2,4-DNP, Supplementary Figure 9, respectively). The OCR and ECAR values were further normalized to the number of cells present in each well, quantified by the Hoechst staining (HO33342; Sigma-Aldrich) as measured using fluorescence at 355 nm excitation and 460 nm emission. Normalization to the total protein amount in these cells was observed to correlate to the same normalization factor as the Hoechst staining (Supplementary Table 4). The baseline OCR and ECAR were defined as the average values measured from time point 1 to 5 (0–45 min) during the experiments. Changes in OCR and ECAR in response to substrates and inhibitors addition were defined as the maximal change after the chemical addition compared with the baseline. Due to variations in the absolute magnitude of OCR and ECAR measurements in different experiments, the relative OCR/ECAR levels were used to compare and summarize independent biological replicates. Calculations were done as the ratio of OCR or ECAR values in EpiSC or hESC compared with ESC.

Mitochondrial membrane potential measurement. ESC and EpiSC were washed with DPBS, and 2 ml of DMEM with 100 nM TMRM (Invitrogen) was added to the culture plate for incubation at 37°C for 30 min. Cells were further trypsinized and resuspended in DPBS for FACS analysis (BD FACS Canto II System). Channel PE was used to detect the fluorescent signal as stained by TMRM.

mtDNA copy number measurement. The ratio of mtDNA to genomic DNA was calculated by dividing copies of Co1 with copies of Gapdh in each experiment. The details of the assay were further described in Supplementary Procedures. Primers are listed in Supplementary Table 6.

ATP turnover and steady-state level measurement. ATP turnover was calculated directly from SeaHorse OCR and PPR measurements following the formula: 1 ATP = 5 × OCR areas under the curve + PPR areas under the curve. The steady-state level cellular ATP was measured following the instruction specified in the ATP Determination Kit (Invitrogen). Briefly, cells were lysed with MPER extraction buffer (Thermo Scientific) in the presence of proteinase inhibitors. Total protein amounts in each reaction were quantified using BCA protein assay (Thermo Scientific).

COX (ETC complex IV) activity assay. ESC and EpiSC were collected and spun down as pellets. Cell lysis, protein extraction and activity measurement followed the instructions specified in Complex IV Rodent Enzyme Activity Microplate Assay Kit (MitoSciences). The details of the assay were further described in Supplementary Procedures.

Isolation of E3.5 ICM and E6.5 epiblast and RNA sequencing. All embryos were recovered from C57BL/6 females. E3.5 blastocysts were flushed from the uterus of superovulated pregnant females. For the isolation of ICM, blastocysts were first placed in a rabbit anti-mouse polyclonal antibody (Rockland Immunochemicals) for 20 min at 37°C and followed by guinea pig serum complement for 20–30 min at 37°C. The lysed trophectoderm cells were removed and the isolated ICM was placed in lysis buffer. The derivation of epiblast from E6.5 post-implantation embryos has been described previously (Brons *et al*, 2007). The detailed RNA-sequencing procedures were described in Supplementary Procedures.

HIF overexpression by retroviral infection and $CoCl_2$ induction. To obtain constitutively stable expression HIF1α protein, non-degradable HIF1α overexpressing plasmid (Addgene plasmid 19005) was used, in which two of the proline sites of HIF1α cDNA were changed to alanine as described previously (Yan *et al*, 2007). Retrovirus made from the plasmid was infected into ESC in the presence of hexadimethrine bromide at 4 ng/ml (Polybrene, Invitrogen) and was changed into normal growth media containing LIF but without 2i after 24 h. Alternatively, $CoCl_2$ (Sigma) was used as a chemical hypoxia inducer to stabilize HIF1α in ESC. For this, 100 μM $CoCl_2$ was provided at the time of plating. ESC were cultured in normal growth medium containing LIF and $CoCl_2$ but without 2i for 3 days before SeaHorse assay or morphology examination. To induce HIF1α expression for a longer term, ESC were first cultured in normal growth media with LIF and $CoCl_2$ (or HIF1α viral expression) but without 2i for 3 days, and then switched to EpiSC media containing Activin and FGF for additional 3 days for further maturation.

HIF1α protein western blot. HIF1α protein stabilization in various pluripotent stages was examined using western blot following procedures specified previously (Zhou *et al*, 2011), and using HIF1α (ab2185; Abcam, Cambridge, MA) at 1:1000 dilution.

Activin/Nodal signalling inhibition. SB431542 (Stemgent) was maintained as a 20-mM stock solution in DMSO (vehicle) and was provided at 20 μM to the cultures at the time of plating and every day thereafter with the media change. ESC were cultured in normal growth media as specified above with SB431542 for 3 days before morphology examination.

Details of lactate measurement of ESC, EpiSC and hESC, RNA isolation and gene expression by real-time, PCR Electron microscopy of mitochondria and quantification of elongated mitochondria were described in Supplementary Procedures.

Supplementary data
Further details of methods and other Supplementary data are available at *The EMBO Journal* Online (http://www.embojournal.org).

Acknowledgements

We thank members of the Ruohola-Baker laboratory for helpful discussions throughout this work. We thank Dr Ian Sweet in the Division of Metabolism, Endocrinology and Nutrition core for experiments using a Perifusion Flow System and Perifusion Microscopic System. We also thank Dr Georgios Karamanlidis for helpful discussions on mitochondrial activity assays and Angel Nelson for help on cell culture of ES cell lines. We thank Dr A Nagy for ESC cell line R1 and G4, and Dr P Tesar for EpiSC cell line #5 and #7. This work was supported by grants from the National Institutes of Health DK17047, DERC Islet Core to IRS, R01DK078340 to MSH, P30 DK056465-11S2 to CW, R01GM083867 to HRB and 1P01GM081619 to CAB, CW and HRB.

Conflict of interest

The authors declare that they have no conflict of interest.

References

Bendall SC, Stewart MH, Menendez P, George D, Vijayaragavan K, Werbowetski-Ogilvie T, Ramos-Mejia V, Rouleau A, Yang J, Bosse M, Lajoie G, Bhatia M (2007) IGF and FGF cooperatively establish the regulatory stem cell niche of pluripotent human cells *in vitro*. *Nature* **448:** 1015–1021

Bertoni-Freddari C, Fattoretti P, Giorgetti B, Solazzi M, Balietti M, Casoli T, Di Stefano G (2004) Cytochrome oxidase activity in hippocampal synaptic mitochondria during aging: a quantitative cytochemical investigation. *Ann NY Acad Sci* **1019:** 33–36

Bracha AL, Ramanathan A, Huang S, Ingber DE, Schreiber SL (2010) Carbon metabolism-mediated myogenic differentiation. *Nat Chem Biol* **6:** 202–204

Brons IG, Smithers LE, Trotter MW, Rugg-Gunn P, Sun B, Chuva de Sousa Lopes SM, Howlett SK, Clarkson A, Ahrlund-Richter L, Pedersen RA, Vallier L (2007) Derivation of pluripotent epiblast stem cells from mammalian embryos. *Nature* **448:** 191–195

Brook FA, Gardner RL (1997) The origin and efficient derivation of embryonic stem cells in the mouse. *Proc Natl Acad Sci USA* **94:** 5709–5712

Camus A, Perea-Gomez A, Moreau A, Collignon J (2006) Absence of Nodal signaling promotes precocious neural differentiation in the mouse embryo. *Dev Biol* **295:** 743–755

Chappell JB, Greville GD (1961) Effects of oligomycin on respiration and swelling of isolated liver mitochondria. *Nature* **190:** 502–504

Cho YM, Kwon S, Pak YK, Seol HW, Choi YM, Park do J, Park KS, Lee HK (2006) Dynamic changes in mitochondrial biogenesis and antioxidant enzymes during the spontaneous differentiation of human embryonic stem cells. *Biochem Biophys Res Commun* **348:** 1472–1478

Dillin A, Hsu AL, Arantes-Oliveira N, Lehrer-Graiwer J, Hsin H, Fraser AG, Kamath RS, Ahringer J, Kenyon C (2002) Rates of behavior and aging specified by mitochondrial function during development. *Science* **298:** 2398–2401

Dunwoodie SL (2009) The role of hypoxia in development of the Mammalian embryo. *Dev Cell* **17:** 755–773

Ehrenberg B, Montana V, Wei MD, Wuskell JP, Loew LM (1988) Membrane potential can be determined in individual cells from the nernstian distribution of cationic dyes. *Biophys J* **53:** 785–794

Evans MJ, Kaufman MH (1981) Establishment in culture of pluripotential cells from mouse embryos. *Nature* **292:** 154–156

Fischer B, Bavister BD (1993) Oxygen tension in the oviduct and uterus of rhesus monkeys, hamsters and rabbits. *J Reprod Fertil* **99:** 673–679

Folmes CD, Nelson TJ, Martinez-Fernandez A, Arrell DK, Lindor JZ, Dzeja PP, Ikeda Y, Perez-Terzic C, Terzic A (2011) Somatic oxidative bioenergetics transitions into pluripotency-dependent glycolysis to facilitate nuclear reprogramming. *Cell Metab* **14:** 264–271

Gan B, Hu J, Jiang S, Liu Y, Sahin E, Zhuang L, Fletcher-Sananikone E, Colla S, Wang YA, Chin L, Depinho RA (2010) Lkb1 regulates quiescence and metabolic homeostasis of haematopoietic stem cells. *Nature* **468:** 701–704

Garrido-Martin EM, Blanco FJ, Fernandez LA, Langa C, Vary CP, Lee UE, Friedman SL, Botella LM, Bernabeu C (2010) Characterization of the human Activin-A receptor type II-like kinase 1 (ACVRL1) promoter and its regulation by Sp1. *BMC Mol Biol* **11:** 51

Goldsby RA, Heytler PG (1963) Uncoupling of oxidative phosphorylation by carbonyl cyanide phenylhydrazones. II. Effects of carbonyl cyanide M-chlorophenylhydrazone on mitochondrial respiration. *Biochemistry* **2:** 1142–1147

Greber B, Wu G, Bernemann C, Joo JY, Han DW, Ko K, Tapia N, Sabour D, Sterneckert J, Tesar P, Scholer HR (2010) Conserved and divergent roles of FGF signaling in mouse epiblast stem cells and human embryonic stem cells. *Cell Stem Cell* **6:** 215–226

Guo G, Yang J, Nichols J, Hall JS, Eyres I, Mansfield W, Smith A (2009) Klf4 reverts developmentally programmed restriction of ground state pluripotency. *Development* **136:** 1063–1069

Hayashi K, Ohta H, Kurimoto K, Aramaki S, Saitou M (2011) Reconstitution of the mouse germ cell specification pathway in culture by pluripotent stem cells. *Cell* **146:** 519–532

Hayashi K, Surani MA (2009) Self-renewing epiblast stem cells exhibit continual delineation of germ cells with epigenetic reprogramming *in vitro*. *Development* **136:** 3549–3556

Heytler PG (1963) uncoupling of oxidative phosphorylation by carbonyl cyanide phenylhydrazones. I. Some characteristics of m-Cl-CCP action on mitochondria and chloroplasts. *Biochemistry* **2:** 357–361

Inman GJ, Nicolas FJ, Callahan JF, Harling JD, Gaster LM, Reith AD, Laping NJ, Hill CS (2002) SB-431542 is a potent and specific inhibitor of transforming growth factor-beta superfamily type I activin receptor-like kinase (ALK) receptors ALK4, ALK5, and ALK7. *Mol Pharmacol* **62:** 65–74

James D, Levine AJ, Besser D, Hemmati-Brivanlou A (2005) TGFbeta/activin/nodal signaling is necessary for the maintenance of pluripotency in human embryonic stem cells. *Development* **132:** 1273–1282

Kamei Y, Ohizumi H, Fujitani Y, Nemoto T, Tanaka T, Takahashi N, Kawada T, Miyoshi M, Ezaki O, Kakizuka A (2003) PPARgamma coactivator 1beta/ERR ligand 1 is an ERR protein ligand, whose expression induces a high-energy expenditure and antagonizes obesity. *Proc Natl Acad Sci USA* **100:** 12378–12383

Krahl ME, Clowes GH (1936) Studies on cell metabolism and cell division: Ii. Stimulation of cellular oxidation and reversible inhibition of cell division by dihalo and trihalophenols. *J Gen Physiol* **20:** 173–184

Lee YM, Jeong CH, Koo SY, Son MJ, Song HS, Bae SK, Raleigh JA, Chung HY, Yoo MA, Kim KW (2001) Determination of hypoxic region by hypoxia marker in developing mouse embryos *in vivo*: a possible signal for vessel development. *Dev Dyn* **220:** 175–186

Lelliott CJ, Medina-Gomez G, Petrovic N, Kis A, Feldmann HM, Bjursell M, Parker N, Curtis K, Campbell M, Hu P, Zhang D, Litwin SE, Zaha VG, Fountain KT, Boudina S, Jimenez-Linan M, Blount M, Lopez M, Meirhaeghe A, Bohlooly YM *et al* (2006) Ablation of PGC-1beta results in defective mitochondrial activity, thermogenesis, hepatic function, and cardiac performance. *PLoS Biol* **4:** e369

Li L, Shen JJ, Bournat JC, Huang L, Chattopadhyay A, Li Z, Shaw C, Graham BH, Brown CW (2009) Activin signaling: effects on body composition and mitochondrial energy metabolism. *Endocrinology* **150:** 3521–3529

Lin J, Handschin C, Spiegelman BM (2005) Metabolic control through the PGC-1 family of transcription coactivators. *Cell Metab* **1:** 361–370

Lux A, Salway F, Dressman HK, Kroner-Lux G, Hafner M, Day PJ, Marchuk DA, Garland J (2006) ALK1 signalling analysis identifies angiogenesis related genes and reveals disparity between TGF-beta and constitutively active receptor induced gene expression. *BMC Cardiovasc Disord* **6:** 13

Mandal S, Lindgren AG, Srivastava AS, Clark AT, Banerjee U (2011) Mitochondrial function controls proliferation and early differentiation potential of embryonic stem cells. *Stem Cells* **29:** 486–495

Nichols J, Smith A (2009) Naive and primed pluripotent states. *Cell Stem Cell* **4:** 487–492

Ojaimi J, Masters CL, McLean C, Opeskin K, McKelvie P, Byrne E (1999) Irregular distribution of cytochrome *c* oxidase protein subunits in aging and Alzheimer's disease. *Ann Neurol* **46:** 656–660

Papadopoulou LC, Sue CM, Davidson MM, Tanji K, Nishino I, Sadlock JE, Krishna S, Walker W, Selby J, Glerum DM, Coster RV, Lyon G, Scalais E, Lebel R, Kaplan P, Shanske S, De Vivo DC, Bonilla E, Hirano M, DiMauro S *et al* (1999) Fatal infantile cardioencephalomyopathy with COX deficiency and mutations in SCO2, a COX assembly gene. *Nat Genet* **23:** 333–337

Ren JC, Rebrin I, Klichko V, Orr WC, Sohal RS (2010) Cytochrome *c* oxidase loses catalytic activity and structural integrity during the aging process in Drosophila melanogaster. *Biochem Biophys Res Commun* **401:** 64–68

Roberts LD, Virtue S, Vidal-Puig A, Nicholls AW, Griffin JL (2009) Metabolic phenotyping of a model of adipocyte differentiation. *Physiol Genomics* **39:** 109–119

Sathananthan AH, Trounson AO (2000) Mitochondrial morphology during preimplantational human embryogenesis. *Hum Reprod* **15** (Suppl 2)**:** 148–159

Seagroves TN, Ryan HE, Lu H, Wouters BG, Knapp M, Thibault P, Laderoute K, Johnson RS (2001) Transcription factor HIF-1 is a necessary mediator of the Pasteur effect in mammalian cells. *Mol Cell Biol* **21:** 3436–3444

Shao D, Liu Y, Liu X, Zhu L, Cui Y, Cui A, Qiao A, Kong X, Chen Q, Gupta N, Fang F, Chang Y (2010) PGC-1 beta-regulated mitochondrial biogenesis and function in myotubes is mediated by NRF-1 and ERR alpha. *Mitochondrion* **10:** 516–527

Smith AG, Heath JK, Donaldson DD, Wong GG, Moreau J, Stahl M, Rogers D (1988) Inhibition of pluripotential embryonic stem cell differentiation by purified polypeptides. *Nature* **336:** 688–690

Sonoda J, Mehl IR, Chong LW, Nofsinger RR, Evans RM (2007) PGC-1beta controls mitochondrial metabolism to modulate circadian activity, adaptive thermogenesis, and hepatic steatosis. *Proc Natl Acad Sci USA* **104:** 5223–5228

Tesar PJ, Chenoweth JG, Brook FA, Davies TJ, Evans EP, Mack DL, Gardner RL, McKay RD (2007) New cell lines from mouse epiblast share defining features with human embryonic stem cells. *Nature* **448:** 196–199

Thomson JA, Itskovitz-Eldor J, Shapiro SS, Waknitz MA, Swiergiel JJ, Marshall VS, Jones JM (1998) Embryonic stem cell lines derived from human blastocysts. *Science* **282:** 1145–1147

Thundathil J, Filion F, Smith LC (2005) Molecular control of mitochondrial function in preimplantation mouse embryos. *Mol Reprod Dev* **71:** 405–413

Vallier L, Reynolds D, Pedersen RA (2004) Nodal inhibits differentiation of human embryonic stem cells along the neuroectodermal default pathway. *Dev Biol* **275:** 403–421

Varum S, Momcilovic O, Castro C, Ben-Yehudah A, Ramalho-Santos J, Navara CS (2009) Enhancement of human embryonic stem cell pluripotency through inhibition of the mitochondrial respiratory chain. *Stem Cell Res* **3:** 142–156

Villani G, Greco M, Papa S, Attardi G (1998) Low reserve of cytochrome *c* oxidase capacity *in vivo* in the respiratory chain of a variety of human cell types. *J Biol Chem* **273:** 31829–31836

Wacker I, Sachs M, Knaup K, Wiesener M, Weiske J, Huber O, Akcetin Z, Behrens J (2009) Key role for activin B in cellular transformation after loss of the von Hippel-Lindau tumor suppressor. *Mol Cell Biol* **29:** 1707–1718

Ware C, Wang L, Mecham BH, Shen L, Nelson AM, Bar M, Lamba DA, Dauphin DS, Buckingham B, Askari B, Lim R, Tewari M, Gartler SM, Issa JP, Pavlidis P, Duan Z, Blau CA (2009) Histone deacetylase inhibition elicits an evolutionarily conserved self-renewal program in embryonic stem cells. *Cell Stem Cell* **4:** 359–369

Whitehouse S, Cooper RH, Randle PJ (1974) Mechanism of activation of pyruvate dehydrogenase by dichloroacetate and other halogenated carboxylic acids. *Biochem J* **141:** 761–774

Wiley M, Sweeney KR, Chan DA, Brown KM, McMurtrey C, Howard EW, Giaccia AJ, Blader IJ (2010) Toxoplasma gondii activates hypoxia-inducible factor (HIF) by stabilizing the HIF-1alpha subunit via type I activin-like receptor kinase receptor signaling. *J Biol Chem* **285:** 26852–26860

Wu Z, Puigserver P, Andersson U, Zhang C, Adelmant G, Mootha V, Troy A, Cinti S, Lowell B, Scarpulla RC, Spiegelman BM (1999) Mechanisms controlling mitochondrial biogenesis and respiration through the thermogenic coactivator PGC-1α. *Cell* **98:** 115–124

Yan Q, Bartz S, Mao M, Li L, Kaelin WG (2007) The hypoxia-inducible factor 2alpha N-terminal and C-terminal transactivation domains cooperate to promote renal tumorigenesis *in vivo*. *Mol Cell Biol* **27:** 2092–2102

Yanes O, Clark J, Wong DM, Patti GJ, Sanchez-Ruiz A, Benton HP, Trauger SA, Desponts C, Ding S, Siuzdak G (2010) Metabolic oxidation regulates embryonic stem cell differentiation. *Nat Chem Biol* **6:** 411–417

Ying QL, Wray J, Nichols J, Batlle-Morera L, Doble B, Woodgett J, Cohen P, Smith A (2008) The ground state of embryonic stem cell self-renewal. *Nature* **453:** 519–523

Zhang H, Gao P, Fukuda R, Kumar G, Krishnamachary B, Zeller KI, Dang CV, Semenza GL (2007) HIF-1 inhibits mitochondrial biogenesis and cellular respiration in VHL-deficient renal cell carcinoma by repression of C-MYC activity. *Cancer Cell* **11:** 407–420

Zhou W, Dosey TL, Biechele T, Moon RT, Horwitz MS, Ruohola-Baker H (2011) Assessment of Hypoxia inducible factor levels in cancer cell lines upon hypoxic induction using a novel reporter construct. *PLoS ONE* **6:** e27460

